HHS Public Access

Author manuscript

Mucosal Immunol. Author manuscript; available in PMC 2017 March 06.

Published in final edited form as:

Mucosal Immunol. 2017 March ; 10(2): 395–407. doi:10.1038/mi.2016.63.

Contribution of mucus concentration and secreted mucins Muc5ac and Muc5b to the pathogenesis of muco-obstructive lung disease

Alessandra Livraghi-Butrico[1], **Barbara R. Grubb**[1], **Kristen J. Wilkinson**[1], **Allison S. Volmer**[1], **Kimberly A. Burns**[1], **Christopher M. Evans**[2], **Wanda K. O'Neal**[#1], and **Richard C. Boucher**[#1]

[1]University of North Carolina Marsico Lung Institute/ Cystic Fibrosis Center, School of Medicine, The University of North Carolina at Chapel Hill, 125 Mason Farm Rd. 27599, Chapel Hill, NC, USA

[2] Department of Medicine, University of Colorado School of Medicine, 12700 E 19th Avenue, Mailstop 8611, Research Complex 2, Room 3121, Aurora, Colorado 80045, USA

[#] These authors contributed equally to this work.

Abstract

Airway diseases, including cigarette smoke-induced chronic bronchitis, cystic fibrosis, and primary ciliary dyskinesia are associated with decreased mucociliary clearance (MCC). However, it is not known whether a simple reduction in MCC or concentration-dependent mucus adhesion to airway surfaces dominates disease pathogenesis or whether decreasing the concentration of secreted mucins may be therapeutic. To address these questions, *Scnn1b*-Tg mice, which exhibit airway mucus dehydration/adhesion, were compared to and crossed with *Muc5b*- and *Muc5ac*-deficient mice. Absence of Muc5b caused a 90% reduction in MCC, whereas *Scnn1b*-Tg mice exhibited an ~50% reduction. However, the degree of MCC reduction did not correlate with bronchitic airways pathology, which was observed only in *Scnn1b*-Tg mice. Ablation of *Muc5b* significantly reduced the extent of mucus plugging in *Scnn1b*-Tg mice. However, complete absence of Muc5b in *Scnn1b*-Tg mice was associated with increased airway inflammation, suggesting that Muc5b is required to maintain immune homeostasis. Loss of Muc5ac had few phenotypic consequences in *Scnn1b*-Tg mice. These data suggest that: (1) mucus

Corresponding author: Alessandra Livraghi-Butrico, PhD, University of North Carolina at Chapel Hill, Marsico Lung Institute/ Cystic Fibrosis Center, Marsico Hall, Rm#7211, 125 Mason Farm Rd, Chapel Hill, NC 27599, Tel: 919-843-1097, Fax: 919-966-5178, alessandra_livraghi@med.unc.edu.

DISCLOSURE

All other authors have no conflict of interest to disclose.

AUTHOR CONTRIBUTION

A.L.-B., W.K.O, and R.C.B. designed the study; K.J.W. and A.S.V. maintained mouse colonies, generated experimental animals, and collected body weight and survival data; A.L.B and K.J.W. performed phenotyping experiments involving BAL analyses (differential cell counts, microbiology, etc.) and tissue harvest; K.A.B. provided histological specimens; A.L.-B. performed mucin agarose western blots, histopathological, immunohistochemistry/immunofluorescence, and morphometric analyses; B.R.G. performed and analyzed the data for the MCC assay; C.M.E., provided $Muc5ac^{-/-}$ and $Muc5b^{-/-}$ mice and review the manuscript; A.L.-B. analyzed the rest of the data, and wrote the manuscript. B.R.G., W.K.O, and R.C.B contributed to interpretation of the data and review the manuscript.

SUPPLEMENTARY MATERIAL: Supplementary Figures 1-8

hyperconcentration dominates over MCC reduction alone to produce bronchitic airways pathology; (2) Muc5b is the dominant contributor to the *Scnn1b*-Tg phenotype; and (3) therapies that limit mucin secretion may reduce plugging, but complete Muc5b removal from airway surfaces may be detrimental.

Keywords

Muc5ac; Muc5b; *Scnn1b*-Tg mouse model; mucociliary clearance; chronic bronchitis

INTRODUCTION

Secretion and clearance of mucus constitute a conserved mechanism for host protection across species. Airway mucus, a heterogeneous mixture of water, mucins, proteins, salts, and lipids, is traditionally listed among lung innate defenses due to its ability to trap and mediate swift removal of inhaled particles/pathogens by mechanical clearance [1]. Effective mucus clearance is essential for respiratory health, as illustrated by the poor prognosis of lung diseases characterized by airway mucus stasis, *e.g.*, cystic fibrosis (CF), primary ciliary dyskinesia (PCD), the bronchitis associated with chronic obstructive pulmonary disease (COPD), and bronchiectasis. Regardless of etiology, all of these bronchitic diseases share the common hallmarks of abnormal sputum production and an airway pathology reflecting epithelial remodeling, mucus accumulation, and inflammation. Increasing efforts have been focused on understanding airway mucus biology and, in particular, how the abnormal structure and function of mucus may produce disease. A complex picture is emerging, where the particular features of diseased mucus might include abnormal concentration ("hydration") [2-4], biogenesis and pH [5-8], macromolecular organization [9,10], and/or functional relationships with other components of the host defense, including inflammatory cells [11-13].

The gel-forming mucins MUC5AC and MUC5B, as well as their murine homologs Muc5ac and Muc5b, are the principal macromolecular components of airway mucus and dominate its biophysical properties[14-16]. Once secreted into the extracellular space, gel-forming mucins are found as mucin/protein complexes with seemingly organized structures [10]. MUC5AC and MUC5B are different in terms of domain structure, glycosylation, assembly, and secretion sites [17], and are thus predicted to have different functions. In humans, cigarette smoke-induced chronic bronchitis, CF, and PCD are characterized predominately by increases in MUC5B, whereas MUC5AC may be the predominant mucin expressed in asthma [3,15,18]. Recent reports have identified Muc5b as essential for mucociliary clearance [19] and Muc5ac hypersecretion as a major determinant of hyperreactivity to inhaled methacoline in allergen-challenged mouse airways[20]. However, the functional significance of these two mucins in the pathogenesis of bronchitic lung diseases remains to be fully elucidated.

Defective mucus clearance has been experimentally generated in *Scnn1b*-transgenic (*Scnn1b*-Tg) mice by airway-targeted overexpression of the epithelial Na^+ channel β subunit (βENaC, encoded by the *Scnn1b* gene)[21]. Expression of the *Scnn1b* transgene causes airway surface dehydration with a consequent increase in mucus concentration, which leads to

osmotic compression of cilia, mucus adhesion, and airway obstruction. As noted above, airway clearance is also reduced in *Muc5b* knock-out (*Muc5b*$^{-/-}$) mice[19], but because these two mouse models have been studied independently, the relative contributions of "low" vs "high" mucin concentration mechanisms that degrade mucus clearance to the pathogenesis of bronchitic lung diseases are unknown.

The overall goal of the present study was to test which specific defect(s) in the mucus clearance system, *i.e.*, mucus hyperconcentration/adhesion as observed in the *Scnn1b*-Tg model, or selective reduction in mucus flow, as observed in the *Muc5b*$^{-/-}$ model, produce the pathologic correlate of bronchitis, *e.g.*, airway remodeling, inflammation, and mucus accumulation. Further, we investigated which of the major secreted mucins (Muc5ac or Muc5b) dominates the muco-obstructive phenotype of *Scnn1b*-Tg mice and whether genetic reductions in mucin concentration might be advantageous. To address these questions, we crossed *Muc5b*$^{-/-}$ mice or *Muc5ac*$^{-/-}$ mice with *Scnn1b*-Tg mice and characterized the phenotype of the progeny.

RESULTS

Survival and body weights of the *Muc5b*$^{-/-}$ × *Scnn1b*-Tg cross progeny

The *Muc5b*$^{-/-}$ × *Scnn1b*-Tg cross generated mice of six different genotypes: *Muc5b*$^{+/+}$, *Muc5b*$^{+/-}$, and *Muc5b*$^{-/-}$ either positive (*Scnn1b*-Tg) or negative for *Scnn1b* overexpression (See Methods for the mouse nomenclature adopted in the main text and legends). *Scnn1b*-Tg mice exhibited only mild lethality compared to WT littermates (**Supplementary Figure 1a**), regardless of their *Muc5b* genotype, as expected for mice in a mixed C57BL/6N [22]:129/SV [23] genetic background. At post-natal day (PND) 35 *Muc5b*$^{-/-}$*Scnn1b*-Tg mice exhibited a slight reduction in body weight as compared to *Muc5b*$^{+/+}$ littermates (**Supplementary Figure 1b,c**), but this finding was not apparent in the progeny of congenic C57 *Muc5b*$^{-/-}$ × *Scnn1b*-Tg mice (**Supplementary Figure 1d-f**) .

Mucus hyperconcentration/adhesion is necessary to produce bronchitic lung pathology

To determine whether mucus hyperconcentration/adhesion or reduced mucus flow *per se* can produce bronchitic lung pathology, we first compared *Muc5b*$^{-/-}$ and *Muc5b*$^{+/+}$*Scnn1b*-Tg mice vs. *Muc5b*$^{+/+}$ littermates. Histologically, *Muc5b*$^{-/-}$ mice were indistinguishable from *Muc5b*$^{+/+}$ littermates (**Figure 1a-c**). In contrast, *Muc5b*$^{+/+}$*Scnn1b*-Tg mice exhibited a severe bronchitic pathology characterized by inflammatory infiltrates, luminal secretions, and emphysematous lesions (Figure 1a-c). Airway mucus content was evaluated histologically with AB-PAS staining (**Figure 1d**) and quantified morphometrically as mucus volume density (mucus V_S, [24]) in the airways (epithelial + lumen, **Figure 1e**) and in the epithelia alone (**Figure 1f**). The mucus content in *Muc5b*$^{+/+}$ and Muc5b$^{-/-}$ mice was minimal, and mostly confined to the intraepithelial compartment (**Figure 1e**). In contrast, *Muc5b*$^{+/+}$*Scnn1b*-Tg mice exhibited substantial intraluminal mucus accumulation, consistent with muco-obstructive lung disease. Secreted mucins were also evaluated by western blots of bronchoalveolar lavage (BAL) (**Figure 1f,g** and **Supplementary Figure 2,** upper panels). Muc5b was absent in *Muc5b*$^{-/-}$ mice, and the Muc5b BAL content was greatly increased in *Muc5b*$^{+/+}$*Scnn1b*-Tg mice, consistent with previous reports[25]. Parallel

quantification of Muc5ac content revealed a modest increase in *Muc5b*$^{-/-}$ mice as compared to *Muc5b*$^{+/+}$ mice (~3 fold, p<0.05. **Figure 1h**), in agreement with previous mRNA and immunohistological data[19]. *Muc5b*$^{+/+}$*Scnn1b*-Tg mice exhibited a significant increase in Muc5ac (~ 18 fold vs. *Muc5b*$^{+/+}$ mice, **Figure 1h**), in agreement with previous mRNA data [24] and suggesting accumulation of Muc5ac due to poor clearance.

Muc5b deletion ameliorates airway mucus obstruction in *Scnn1b*-Tg mice

The effect of *Muc5b* genetic deletion on the phenotype of *Scnn1b*-Tg mice was evaluated by comparing *Muc5b*$^{-/-}$*Scnn1b*-Tg and *Muc5b*$^{+/-}$*Scnn1b*-Tg mice vs. *Muc5b*$^{+/+}$*Scnn1b*-Tg littermates. Histologically, all three genotypes exhibited prominent airway inflammation (**Figure 1a,b**) and parenchymal remodeling (**Figure 1a,c**)

Notably, *Muc5b*$^{-/-}$*Scnn1b*-Tg mice exhibited a significant reduction in intraluminal mucus as compared to *Muc5b*$^{+/+}$*Scnn1b*-Tg mice, but secretions adherent to airway surfaces were still detected (**Figure 1d,e**). A genotype-dependent reduction in BAL Muc5b content was noted in the *Muc5b*$^{+/-}$*Scnn1b*-Tg and *Muc5b*$^{-/-}$*Scnn1b*-Tg mice (**Figure 1g**), reflecting allelic insufficiency and complete deletion of *Muc5b*, respectively. Also, there was a genotype-dependent increase in BAL Muc5ac content in *Muc5b*$^{-/-}$*Scnn1b*-Tg mice (~ 46 fold vs. *Muc5b*$^{+/+}$ mice and ~ 2.5 fold vs. *Muc5b*$^{+/+}$*Scnn1b*-Tg mice, **Figure 1h**), likely contributing to the residual mucus observed in the airways (**Figure 1d**).

Muc5ac deletion does not ameliorate airway mucus obstruction in *Scnn1b*-Tg mice

Initial crosses between *Muc5ac*$^{-/-}$ and *Muc5ac*$^{+/-}$*Scnn1b*-Tg mice in the C57:129 background generated mice of four different genotypes *(Muc5ac*$^{+/-}$; *Muc5ac*$^{-/-}$; *Muc5ac*$^{+/-}$*Scnn1b*-Tg; *and Muc5ac*$^{-/-}$*Scnn1b*-Tg) in the expected Mendelian proportions, and all exhibited high survival (**Supplementary Figure 3a**). Analyses performed on the progeny of congenic C57BL/6N mice bred to generate all six possible genotypes (*Muc5ac*$^{+/-}$ × *Muc5ac*$^{+/-}$*Scnn1b*-Tg) confirmed that *Muc5ac* deletion did not significantly affect survival (**Supplementary Figure 3b**)or body mass (**Supplementary Figure 3c,d**).

Similar to the cross with *Muc5b*$^{-/-}$ mice, only *Scnn1b*-Tg mice exhibited bronchitic lung pathology when evaluated on H&E stained sections, regardless of *Muc5ac* genotype (not shown). However, in contrast to what was observed for the *Muc5b*$^{-/-}$ cross, there were no differences in AB-PAS positive mucus content, either luminal or epithelial, between *Muc5ac*-deficient or sufficient *Scnn1b*-Tg mice (**Figure 2a-c**). These data suggest that Muc5ac did not significantly contribute to the intraluminal mucus plugging observed in *Scnn1b*-Tg mice. Quantitation of BAL mucin content (**Figure 2d,e** and **Supplementary Figure 2**, lower panels) revealed that, contrary to *Muc5b*$^{-/-}$ mice, *Muc5ac*$^{-/-}$ mice did not exhibit a compensatory increase in Muc5b compared to *Muc5ac*$^{+/+}$ mice. Muc5b signal was increased in *Scnn1b*-Tg mice, regardless of *Muc5ac* genotype. As for Muc5ac BAL content, the signal for *Muc5ac*$^{+/+}$ and *Muc5ac*$^{+/-}$ mice was just above background, but an increased level of Muc5ac was observed in *Muc5ac*$^{+/+}$*Scnn1b*-Tg mice. Of note, there was a genotype-dependent reduction of harvested Muc5ac in *Muc5ac*$^{+/-}$*Scnn1b*-Tg and *Muc5ac*$^{-/-}$*Scnn1b*-Tg mice, reflecting the *Muc5ac* allelic make-up of the mice.

Relative contribution of Muc5ac vs. Muc5b to neonatal survival in a model of lethal mucus obstruction, the F1 C57:FVB *Scnn1b*-Tg mouse

As previously reported, the severity of the *Scnn1b*-Tg muco-obstructive phenotype is proportional to airway mucin secretory capacity, which is age- and mouse strain-dependent[22]. Specifically, we and others have reported that neonatal mice experience a transient increase in Muc5ac and Muc5b secretion during the early postnatal period (PND5-10)[25,26]. The developmentally regulated increase in mucin concentration on airway surfaces, coupled to the small caliber of neonatal airways, makes *Scnn1b*-Tg pups more sensitive to the impact of salt and water depletion produced by *Scnn1b*-Tg overexpression and causes fatal tracheal mucus obstruction. We have previously described a variant of *Scnn1b*-Tg mice, F1 C57:FVB *Scnn1b*-Tg mice[22], characterized by extremely high postnatal mortality (90%) and higher BAL mucus content as compared to congenic C57BL/6N *Scnn1b*-Tg mice.

Accordingly, we crossed $Muc5ac^{-/-}$ *Scnn1b*-Tg mice or $Muc5b^{-/-}$ *Scnn1b*-Tg mice with inbred FVB/NJ mice to obtain mice of four different genotypes ($Muc^{+/+}$, $Muc^{+/-}$, $Muc^{+/+}$ *Scnn1b*-Tg, $Muc^{+/-}$ *Scnn1b*-Tg) in a homogeneous F1 C57:FVB genetic background. The effect of decreased Muc5ac or Muc5b concentration on survival was evaluated. $Muc5b^{+/+}$ and $Muc5b^{+/-}$ mice had the expected normal, high survival, whereas $Muc5b^{+/+}$ *Scnn1b*-Tg mice were all dead within seven days from birth (**Figure 3a**). Importantly, heterozygosity for *Muc5b* significantly improved the survival of $Muc5b^{+/-}$ *Scnn1b*-Tg mice (~70% at PND10) as compared to $Muc5b^{+/+}$ *Scnn1b*-Tg mice (~0% at PND10). When similar studies were performed with $Muc5ac^{-/-}$ mice, we observed no protection from lethality (**Figure 3b**) but a modest though significant delay in mortality of the $Muc5ac^{+/-}$ *Scnn1b*-Tg mice as compared to $Muc5ac^{+/+}$ *Scnn1b*-Tg mice. Collectively, these data suggest that Muc5b is the dominant mucin that leads to lethality of *Scnn1b*-Tg mice in the “high mucus producer” FVB background.

Mucociliary transport only partially correlates with the severity of muco-obstructive lung disease

A key measurement that has been used to relate airway mucus function to disease has been the rate of mucociliary clearance (MCC)[2]. Accordingly, we compared the relative rates of mucus transport in the two models of defective airway clearance, *i.e.*, *Scnn1b*-Tg and $Muc5b^{-/-}$ mice. Furthermore, to test whether a reduction in mucin concentration in the lungs of *Scnn1b*-Tg mice produced by absence of Muc5b might rescue mucus transport, we also measured MCC in $Muc5b^{-/-}$ *Scnn1b*-Tg.

As shown in **Figure 4**, $Muc5b^{+/+}$ mouse lungs cleared ~75% of the tracer particles within 15 minutes after instillation. In contrast, there was almost a complete loss of MCC in $Muc5b^{-/-}$ mice, as previously reported[19]. Also similar to previous reports[21], a ~50% reduction in MCC was observed in $Muc5b^{+/+}$ *Scnn1b*-Tg mice. Notably, deletion of Muc5b in *Scnn1b*-Tg mice did not rescue mucus transport, but rather caused a reduction in MCC towards the levels exhibited by $Muc5b^{-/-}$ mice.

Deletion of Muc5b or Muc5ac does not affect bacterial burden or ameliorate airway inflammation in *Scnn1b*-Tg mice

Because both *Scnn1b*-Tg and *Muc5b*$^{-/-}$ mice have increased susceptibility to spontaneous and experimentally induced airway bacterial infection[19,21,27], we tested whether the combination of the two genotypes would produce an additive phenotype. As effects of Muc5ac deletion on intestinal pathogen clearance have also been reported [28], microbiology experiments were also performed for the *Muc5ac*$^{-/-}$ × *Scnn1b*-Tg cross.

At PND5 7, *Muc5b*$^{-/-}$ mice exhibited an incidence of infection of ~50% compared to 0% in *Muc5b*$^{+/+}$ mice, with a bacterial burden of ~1.5 Log CFU/mouse (**Figure 5a**). In contrast, virtually all neonatal *Scnn1b*-Tg mice were infected with a bacterial burden of ~3 Log CFU/mouse, and this infection was not affected by the *Muc5b* genotype. At PND35, none of the *Muc5b*$^{-/-}$ mice were infected, and sporadic infections were detected in *Scnn1b*-Tg mice (**Figure 5b)**, in agreement with previous reports[27]. Similar to neonatal *Scnn1b*-Tg mice, there was no appreciable difference in bacterial burden due to *Muc5b* genotype in adult WT or *Scnn1b*-Tg mice. A similar picture emerged from the microbiological analysis of BAL samples harvested from mice derived from *Muc5ac*$^{-/-}$ × *Scnn1b*-Tg crosses at PND5 7 (**Supplementary Figure 4**), with the notable exception that *Muc5ac*$^{-/-}$ neonatal mice did not exhibit the incidence of spontaneous bacterial infection observed in neonatal *Muc5b*$^{-/-}$ mice.

To test whether genetic ablation of Muc5ac or Muc5b affected the airway inflammatory profile of *Scnn1b*-Tg mice, we characterize BAL cells in neonatal (PND5 7) and adult (PND35) mice. Neutrophil counts were elevated in both *Muc5b*$^{-/-}$ and *Muc5b*$^{+/+}$*Scnn1b*-Tg neonatal mice as compared to *Muc5b*$^{+/+}$ littermates (**Figure 5c**), in agreement with the presence of bacteria. Rather than rescuing this phenotype, *Muc5b* deletion caused a trend towards worsening of the neutrophil infiltration in *Scnn1b*-Tg mice. In adult mice, there was a modest but significant increase in neutrophil count in *Muc5b*$^{-/-}$ mice, whereas the neutrophil infiltrate was much greater in *Muc5b*$^{+/+}$*Scnn1b*-Tg mice (**Figure 5d**). However, the airway neutrophilia typical of adult *Scnn1b*-Tg mice was not ameliorated by either partial (*Muc5b*$^{+/-}$*Scnn1b*-Tg mice) or total (*Muc5b*$^{-/-}$*Scnn1b*-Tg mice) ablation of Muc5b. Rather, a gene-dosage dependent trend towards worsening of airway neutrophilia was observed (*Muc5b*$^{+/+}$ > *Muc5b*$^{+/-}$ > *Muc5b*$^{-/-}$). Muc5b deletion alone was not associated with significant changes in macrophage numbers either in neonatal (**Supplementary Figure 5a**) or adult WT mice (**Supplementary Figure 5b**). Neonatal *Scnn1b*-Tg mice exhibited a modest increase in BAL macrophages as compared to WT littermates, regardless of *Muc5b* genotype, but this increase was normalized in adult mice with only the *Muc5b*$^{-/-}$*Scnn1b*-Tg mice exhibiting a significant difference versus WT littermates.

As a parallel readout of airway inflammation, we evaluated the BAL chemokine and cytokine profiles in adult mice. The neutrophil chemoattractant chemokines (C-X-C motif) ligand 1 (CXCL1 or KC) and lipopolysaccharide-induced CXC chemokine (LIX) were significantly elevated in *Scnn1b*-Tg mice as compared to both WT and *Muc5b*$^{-/-}$ mice (**Figure 6a,b**). Genetic deletion of *Muc5b* did not alter the levels of these inflammatory markers in *Scnn1b*-Tg mice. Although it did not reach significance, macrophage

inflammatory protein (MIP)-2 was elevated in all *Scnn1b*-Tg samples, regardless of *Muc5b* genotype (**Supplementary Figure 5c)**, whereas IL-6 and TNFα were below the lower limit of detection in all samples (data not shown).

As for the progeny of the *Muc5ac*$^{-/-}$ × *Scnn1b*-Tg cross, partial or total Muc5ac deletion did not cause neutrophilia or altered BAL macrophage counts in either neonatal (**Supplementary Figure 6a,c**) or adult (**Supplementary Figure 6b,d**) WT mice. Of note, Muc5ac deletion did not rescue the BAL neutrophilia in either neonatal or adult *Scnn1b*-Tg mice (**Supplementary Figure 6a,b)**, and only a slight increase in BAL macrophage numbers was detected in neonatal *Muc5ac*$^{-/-}$ *Scnn1b*-Tg mice as compared to WT littermates (**Supplementary Figure 6d)**.

Deletion of Muc5b, but not Muc5ac, worsens the incidence of bronchus-associated lymphoid tissue (BALT) in *Scnn1b*-Tg mice

Histopathological analysis of lung sections stained with hematoxylin and eosin (H&E, **Figure 7a**) using a semi-quantitative score[25] (**Supplementary Figure 7a,b**) and quantitative morphometry (**Figure 7b**) indicated that BALT was absent in PND35 WT mice, regardless of *Muc5ac* or *Muc5b* genotype, whereas low level accumulation of this ectopic lymphoid tissue could be detected in mucin-sufficient *Scnn1b*-Tg mice at this time point. Of note, Muc5b deletion significantly increased the incidence of BALT in *Scnn1b*-Tg mice, whereas Muc5ac deletion did not modify this phenotype. This increase in BALT was not reflected in the total number of BAL lymphocytes, which was elevated in *Scnn1b*-Tg mice regardless of *Muc5b* genotype (**Figure 7c**). Both B and T cells were present in these lymphoid nodules (**Figure 7d**), and their rather loose organization suggested recently formed, inducible BALT[29].

We sought to determine if there was a correlation between incidence of BALT and immunoglobulin concentrations in BAL harvested from the progeny of the *Muc5b*$^{-/-}$ × *Scnn1b*-Tg cross. A striking increase in IgA was observed in all *Scnn1b*-Tg samples, regardless of *Muc5b* genotype (**Figure 8a**). Except for an increase in IgG_1 in *Muc5b*$^{-/-}$ *Scnn1b*-Tg mice (**Figure 8b**), no systematic differences were observed for other IgG subtypes or IgM as a function of Muc5b genotype (**Supplementary Figure 8a-d**). Longitudinal studies comparing *Scnn1b*-Tg and WT littermates showed that IgA levels are increased in the BAL of *Scnn1b*-Tg mice beginning at PND10 (**Supplementary Figure 8e).** Since it has been proposed that IgA binding to mucus through the polymeric Ig receptor secretory component (SC) is essential for IgA function in the lung[30], we tested whether selective deletion of Muc5b or Muc5ac would modify the localization of SC in WT or *Scnn1b*-Tg mice. As shown in **Figure 8c**, SC was exclusively localized to the surface epithelium in both *Muc5b*$^{+/+}$ and *Muc5b*$^{-/-}$ mice (as well as *Muc5ac*$^{-/-}$ mice, not shown), whereas it was abundant in the luminal mucous secretions of *Scnn1b*-Tg mice, and its localization was not altered in the absence of either Muc5ac or Muc5b.

DISCUSSION

Many aspects of lung mucus biology have become better defined in recent years. For example, it appears that Muc5b, not Muc5ac, is the dominant mucin that confers to the

mucus layer the properties required for transport in the healthy lung [19]. Moreover, the dominant role of mucins in producing the biophysical properties governing mucus flow in health versus reduced/no flow in disease has also become better appreciated. Notably, a novel paradigm posits that healthy airway surfaces are populated by two mucus hydrogel layers, one comprised of the mobile layer (where Muc5b is dominant) and the other comprised of the periciliary layer, enriched in tethered mucins including Muc1, Muc4, and Muc16 [4]. The identification of this two-gel topology for the airway surface [9] is key to quantify biophysical variables related to the distribution of water between the two hydrogels, which ultimately determines the efficiency of mucus transport [4]. Of particular relevance for this study is the notion that mucus clearance is inversely proportional to its concentration, a concept recently translated to the clinic [2].

It is clear that mucins play an important role in the pathogenesis of bronchitic lung diseases, which are clinically characterized by increased sputum production over defined periods of time, and pathologically associated with airway epithelial remodeling, including goblet cell metaplasia, inflammation and mucus plugging. Despite the likely importance of mucus in the pathogenesis of these diseases, it is not clear whether abnormal qualitative or quantitative properties of mucus produce disease. Specifically, it is not clear whether the simple absence of mucus clearance, abnormal ratios of MUC5AC to MUC5B, or abnormal mucus concentration are required features to initiate pathology. Heretofore it has been difficult to experimentally separate the two different pathologic mechanisms, *e.g.,* absence of transport versus presence of hyperconcentration, which is key to address this question.

Recently, the opportunity to study the role of mucins subtypes, mucus concentration, and mucus transport in the pathogenesis of bronchitic lung disease has been afforded by the generation of mouse models that produced different perturbations of airway mucus biology. Specifically, the availability of *Muc5b*$^{-/-}$ mice, which exhibit very slow airway mucus transport[19], and *Scnn1b*-Tg mice, which exhibit airway mucus hyperconcentration and adhesion to airway surfaces[21], has provided the opportunity to assess the relative roles and possible interactions of these dysfunctions in a common cohort.

In the studies reported here, the progenies from the mucin deficient × *Scnn1b*-Tg mice crosses were compared utilizing metrics of bronchitic disease severity. Mucin-sufficient *Scnn1b*-Tg mice exhibited a relatively severe bronchitic phenotype, including: 1) increased airway mucus burden (**Figure 1 and 2**); 2) highly penetrant spontaneous bacterial infection (**Figure 5**); 3) significant inflammatory infiltrates (**Figure 5**); 4) epithelial/parenchymal remodeling (**Figure 1 and 7**); and 5) increased in pro-inflammatory cytokines (**Figure 6**) consistent with previous reports [24,25,27]. Novel to this study, we observed another index of increased immune responses, *i.e.,* high concentrations of IgA in *Scnn1b*-Tg BALF (**Figure 7e**). In contrast, *Muc5b*$^{-/-}$ mice exhibited a milder disease, with a lesser incidence of bacterial infection, fewer BAL neutrophils, lower levels of pro-inflammatory cytokines and IgA, and importantly no histological evidence of airway epithelial remodeling or emphysema. In parallel, no evidence of spontaneous lung disease was observed in *Muc5ac*$^{-/-}$ mice, consistent with previous reports[20].

Interestingly, the severity of the obstructive and inflammatory airway phenotype did not simply reflect the rates of airway mucus clearance. As shown in **Figure 4**, airway mucociliary clearance in *Muc5b*$^{-/-}$ mice was indeed lower than in *Scnn1b*-Tg mice, despite the milder phenotype of the former. Accordingly, we speculate that it is not a reduction in the absolute rate of mucus clearance that dominates the pathogenesis of bronchitis, but it is the presence of hyperconcentrated mucus adherent to the airway surfaces, as evident in *Scnn1b*-Tg mice (**Figures 1, 2 and 7**). This interpretation is consistent with findings in other mouse models that exhibit defective mucus transport but lack a mucus-adhesive component, *e.g.*, models of primary ciliary dyskinesia (PCD), which also exhibit a mild lower airway phenotype [3133].

Crossing the *Muc5b*$^{-/-}$ and *Muc5ac*$^{-/-}$ mice with *Scnn1b*-Tg mice also offered the opportunity to query the role of the two major secreted mucins in the development of the *Scnn1b*-Tg phenotype. Muc5ac-deficient *Scnn1b*-Tg mice exhibited little/no change as compared to Muc5ac-sufficient *Scnn1b*-Tg mice (**Figure 2**). In contrast, the magnitude of mucus obstruction in *Scnn1b*-Tg mice was significantly reduced in the absence of Muc5b, as evaluated both morphometrically and by BAL western blot (**Figure 1e,f,g,h**), consistent with the notion that Muc5b is the major secreted mucin in mouse airways [19,26,34]. Despite the reduction in mucus burden, areas of mucus adhesion persisted histologically (**Figure 1d,e**). These plugs likely contained Muc5ac, consistent with the significant accumulation of Muc5ac in the BAL fluid of *Muc5b*$^{-/-}$*Scnn1b*-Tg mice (**Figure 1h**).

The availability of a mouse strain that exhibits a lethal muco-obstructive phenotype, *i.e.*, F1 C57:FVB *Scnn1b*-Tg mice, allowed us to investigate whether decreased levels of Muc5b or Muc5ac could rescue survival. Heterozygosity for Muc5b, but not Muc5ac, was sufficient to significantly rescue the survival of F1 C57:FVB *Scnn1b*-Tg mice (**Figure 3**). Based on the data that *Muc5b*$^{+/-}$*Scnn1b*-Tg mice exhibit ~50% the levels of BAL Muc5b as compared to *Muc5b*$^{+/+}$*Scnn1b*-Tg mice (**Figure 1g**), it is likely that the reduction of Muc5b was responsible for the large increase in survival. In contrast, *Muc5ac*$^{+/-}$*Scnn1b*-Tg mice exhibited a modest increase in time to death as compared to *Muc5ac*$^{+/+}$*Scnn1b*-Tg mice, suggesting that a Th2- or developmentally-driven increase in Muc5ac might be detrimental to survival early in life.

Importantly, inflammation in *Muc5b*$^{-/-}$*Scnn1b*-Tg mice was not reduced proportionately to mucus obstruction. Instead, there was an overall increase in the severity of pulmonary inflammation as indexed by increased number of BAL neutrophils and BALT (**Figures 5 and 7**), These findings suggest that other factors in addition to mucus obstruction can lead to pulmonary inflammation. Perhaps the simplest explanation for the increased inflammatory phenotype in *Muc5b*$^{-/-}$*Scnn1b*-Tg mice is that reduction of secreted Muc5b did not rescue the defective airway clearance of *Scnn1b*-Tg mice but, rather, further reduced mucus clearance to the levels of *Muc5b*$^{-/-}$ mice (**Figure 4**). This reduction could promote further adhesion of other mucus components, possibly Muc5ac, to airway surfaces as well as prolong the residence time of pro-inflammatory particles or debris initiating a predictable inflammatory response. Alternatively, it has been reported that mucins may “communicate” with inflammatory cells, including macrophages and dendritic cells [12,13,3537], and perhaps the absence of Muc5b contributed *per se* to an exaggerated inflammatory response in

Muc5b$^{-/-}$ *Scnn1b*-Tg mice. Finally, gel-forming mucins, and particularly Muc5b, are associated with a network of proteins forming macromolecular complexes, known as “mucin interactomes”, which are thought to be involved in maintaining airway immune homeostasis through their anti-microbial/anti-inflammatory/anti-oxidant functions[38,39]. Derangement of this network may have adverse effects in controlling airway inflammation.

Another unexpected finding of this study was that Muc5b deletion did not affect bacterial burden in *Scnn1b*-Tg mice (**Figure 5a,b**) despite a reduction in mucus plugs. A possible interpretation is that while Muc5b deletion decreased mucus plugging, it also reduced clearance of inhaled bacteria (as indicated by the presence of bacteria in 50% of the neonatal *Muc5b*$^{-/-}$ mice), offsetting the beneficial effect of reduced plugging. We can also speculate that the composition of neonatal mucus, enriched in Muc5ac as compared to adult mice ([26] and A. Livraghi-Butrico, unpublished data), might also contribute to increased, Muc5b-independent trapping of bacteria.

As noted above, we found that IgA BAL levels were elevated in *Scnn1b*-Tg mice, suggesting that mucus hyperconcentration/adhesion stimulates local IgA production and secretion. IgA levels were elevated independently of Muc5b genotype, suggesting that the residual degree of mucus obstruction was sufficient to stimulate IgA synthesis and secretion. Importantly, previous reports have shown that SC-mediated binding of IgA to mucus is required for its function[30]. Our immunohistological data (**Figure 8c**) suggest that SC binding to the mucus is not Muc5ac- or Muc5b-dependent. However, we can not rule out the possibility that the overall decrease in intraluminal Muc5b in *Muc5b*$^{-/-}$ *Scnn1b*-Tg mice removed an essential “scaffold” for secreted IgA, impairing immune exclusion [40] and promoting inflammation.

In conclusion, mucus biology in the normal and diseased lung is complex and likely involves not only the biophysical contributions of mucins to mucus transport but also interactions with host immune cells and defense proteins. Our data suggest that mucus hyperconcentration/adhesion rather than the loss of mucus flow dominates the pathophysiology of bronchitic lung diseases, and, consequently, these diseases may be characterized as “muco-obstructive” lung diseases. So, what is pathogenic in static/adherent mucus? Mucus adhesion certainly blocks airflow, and it is in part responsible for the reduced airflow observed in muco-obstructive lung diseases. Adherent mucus is also the site of most bacterial airways infections, including those causing exacerbations in CF and COPD, and, even when “sterile”, it appears to be a pro-inflammatory DAMP[27]. Moreover, mucus plugging induces local, epithelia hypoxia[24], which is an increasingly recognized feature of the CB syndrome[41], important for both inflammatory responses and anaerobic infection. Notably, therapies designed to clear mucus from airway surfaces are predicted to be therapeutic for these conditions. The simplest therapies involve the “rehydration” of mucus so that its concentration is restored to levels compatible with transport. It is also likely that therapies designed to reduce mucin secretion, and thus reduce concentrations, may also be useful. However, our data suggest that a complete loss of secreted mucins, especially MUC5B, may worsen pathology, so a more moderate titration might be needed therapeutically.

METHODS

Animals

Animals were maintained and studied under protocols approved by the University of North Carolina Institutional Animal Care and Use Committee, according to the principles outlined by the Animal Welfare and the National Institutes of Health guidelines. Mice were housed in individually ventilated micro-isolator cages in a specific pathogen-free facility at the University of North Carolina at Chapel Hill, on a 12-hour day/night cycle. Mice were fed a regular chow diet and given water *ad libitum*.

Muc5ac$^{-/-}$ [20] and *Muc5b*$^{-/-}$ [19] mice were obtained from the Laboratory of Dr. Christopher Evans as C57BL/6J:129/Sv line. Congenic C57BL/6N *Scnn1b*-Tg mice and wild-type (WT) littermates were maintained as a hemizygous as described [22] and referred to as WT (*i.e.,* *Scnn1b-Tg*$^{-}$ or *Scnn1b*-Tg negative) or *Scnn1b*-Tg (*i.e.,* *Scnn1b-Tg*$^{+}$ or *Scnn1b*-Tg positive). Mucin-deficient *Scnn1b*-Tg mice and appropriate littermate controls were generated by sequential breeding of congenic C57BL/6N hemizygous *Scnn1b*-Tg mice with *Muc5ac*$^{-/-}$ or *Muc5b*$^{-/-}$ mice, using a breeding strategy previously described [25]. For clarity, genotypes of the progenies are indicated in the main text and figure legends as follows: *Muc5ac*$^{+/+}$/*Scnn1b-Tg*$^{-}$ = *Muc5ac*$^{+/+}$; *Muc5ac*$^{+/-}$/*Scnn1b-Tg*$^{-}$ = *Muc5ac*$^{+/-}$; *Muc5a*$^{-/-}$/*Scnn1b-Tg*$^{-}$ = *Muc5ac*$^{-/-}$; *Muc5ac*$^{+/+}$/*Scnn1b-Tg*$^{+}$ = *Muc5ac*$^{+/+}$ *Scnn1b*-Tg; *Muc5ac*$^{+/-}$/*Scnn1b-Tg*$^{+}$ = *Muc5ac*$^{+/-}$ *Scnn1b*-Tg; *Muc5a*$^{-/-}$*;Scnn1b-Tg*$^{+}$ = *Muc5ac*$^{-/-}$ *Scnn1b*-Tg; and similarly for the *Muc5b*$^{-/-}$ × *Scnn1b*-Tg cross. Congenic C57BL/6N *Muc5ac*$^{-/-}$ and *Muc5b*$^{-/-}$ mice were generated by crossing heterozygous mice to inbred C57BL/6N mice (Taconic, Hudson, NY) for more than 12 generations. Mixed-strain or congenic mice were used as described in the text. At post-natal day (PND) 1 or 2, pups were toe clipped for identification and genotyping, as previously described [21]. Mice studied were littermates, age-matched and of both sexes. Congenic FVB/NJ mice were purchased from The Jackson Laboratory (Bar Harbor, Maine).

Bronchoalveolar lavage (BAL), cell counts, analyses of soluble contents and bacteriology

BAL was performed in neonatal and adult mice as previously described [25]. For microbiology studies, BAL was performed aseptically and colony forming units (CFUs) enumerated were enumerated in serially plated dilutions [plated onto Columbia anaerobe sheep blood agar (Becton Dickinson, NJ) and incubated in a candle jar to facilitate the growth of microaerophilic bacteria at 37°C for 24 hours], as previously described [27]. Mouse TNFα, KC, MIP-2, LIX, IL-6, IgG_1, IgG_{2a}, IgG_{2b}, IgG_3, IgA, and IgM were measured in cell-free BAL using a Luminex-based assay (EMD Millipore, Billerica, MA), according to the manufacturer's instructions.

Lung histology

Lungs were immersion-fixed in 10% neutral-buffered formalin (NBF) to prevent dislodging of airway luminal contents. Paraffin-embedded sections were stained with hematoxylin and eosin (H&E) and Alcian Blue-Periodic Acid Schiff staining (AB-PAS), and lung pathology graded as previously described using a semi-quantitative histology score [25] or

morphometry[24]. Tissue blocks received a numerical code at time of embedding and scoring was performed by an investigator blinded to specimen genotype.

Agarose gel mucin western blot

Secreted mucin quantification was carried out using a slight modification of the protocol described in [25]. BAL samples were solubilized by addition of urea to reach a 6M concentration. Samples were reduced with 10 mM dithiothreithol for 90 min at 37°C and alkylated with 25 mM iodoacetamide for 30 min at room temperature (RT) in the dark. Equal volumes of reduced samples (40 μl) were run on 1% agarose gel at 80 V for 90 min. Gels were vacuum-blotted onto nitrocellulose membranes with 4x sodium citrate buffer (SSC) for 2 hours, blocked with Odyssey blocking buffer (OBB, Li-COR Biosciences, Lincoln, NE), and probed with rabbit polyclonal antibodies against Muc5b (UNC223, 1:2000 in OBB[34]) or Muc5ac (UNC294, 1:1000 in OBB+0.1% Tween-20, [42]). The secondary antibody was IRDye 680LT donkey anti-rabbit IgG (Li-COR Biosciences), diluted 1:15,000 in OBB. Detection and densitometry were performed using the Odyssey Infrared Imaging System (LI-COR Biosciences).

Mucociliary clearance (MCC) assay

PND35 mice were anesthetized with 2-3 % isoflurane and a small incision was made through the tracheal ventral wall. Using a fine-bore cannula, 200 nl of PBS containing a known number of fluorescent microspheres (3 μm Molecular Probes FluoSpheres, Nile Red, Invitrogen Corp.) was deposited near the tracheal bifurcation. After the cannula was removed and the tracheostomy closed, the anesthetized mouse was allowed to breath spontaneously for 15 minutes. After this period, the mouse was euthanized, the lungs and trachea (up to the larynx) were removed and solubilized in KOH, and the beads left in the tissue were counted. MCC was determined as % of delivered beads that were cleared.

Immunofluorescence analysis of BALT

Lungs were inflated with a 1:1 mixture of OCT:PBS, embedded in 100% OCT and sectioned. Slides were air dried, fixed in ice cold 100% acetone for 5 min, and washed in PBS. Blocking was performed in 5% normal goat serum (NGS, Jackson ImmunoResearch Laboratories Inc., West Grove, PA), 1:50 Fc Block (BD Biosciences, rat anti-mouse CD16/CD22 clone 2.4G2), 0.1% Tween-20, and 0.1% Triton-X in PBS, for 30 min at RT. Primary antibodies and isotype controls [goat anti-mouse CD3-ε (M-20) Santa Cruz and goat IgG Jackson ImmunoResearch 0.2 mg/ml, dil. 1:100; rat anti-mouse CD45R/B220 and rat IgG2a, κ both from BD Biosciences, dil. 1:50] were diluted in PBS + 0.1% Tween-20 + 0.1% Triton-X (PBS-TT) and incubated over night at 4°C. Sections were washed in PBS + 0.1% Tween-20 (PBST) and secondary antibodies (donkey anti-goat AlexaFluor 633 and donkey anti-rat AlexaFluor 594, Jackson ImmunoResearch, both at 1:200 dilution in PBSTT) were applied for 60 min at RT in the dark. After washing in PBST, slides were mounted with Vectashield Soft Mount media (Vector laboratories) containing DAPI for nuclear staining, and imaged by confocal microscopy, using a Leica SP2 microscope with an Apochromat 40x/1.25 NA oil immersion lens.

Immunohistochemical localization of SC

Lungs were immersion fixed in 10% NBF for 24 hours. Paraffin embedded sections were incubated at 65°C for 2-4 hours, and deparaffinized with xylene (2 changes × 5') and graded ethanol (100% 2 × 5', 95% 1 × 5', 70% 1 × 5'). After rehydration, antigen retrieval was performed by boiling the slides in 0.1M sodium citrate pH 6.00 (3 cycles with microwave settings: 100% power for 6.5 min, 60% for 6 min, and 60% for 6 min, refilling the Coplin jars with deionized water after each cycle). After cooling and rinsing with dH_2O, quenching of endogenous peroxidase was performed with 0.5% H_2O_2 in methanol for 15 min, slides were washed in PBS, and blocked with 5% normal donkey serum (NDS), 1:50 Fc block in PBS-T, for 1 hr at RT. Primary antibodies and isotype control (goat anti-mouse pIgR R&D Systems AF2800 and goat IgG Jackson ImmunoResearch 0.2 mg/ml) were diluted in 5% NDS in PBST and incubated over night at 4°C. Sections were washed in PBS and secondary antibody (biotinylated donkey anti-goat IgG, Jackson ImmunoResearch, at 1:200 dilution in 5% NDS in PBST) was applied for 30 min at RT. After washing in PBST, slides were incubated with avidin-peroxidase complex according to the manufacturer instruction (Vectastain kit, Vector laboratories), washed, incubated with the chromogenic substrate (Immpact Novared, Vector laboratories) and counterstained with Mayer hematoxylin. Coverslipped slides were imaged by transmitted light microscopy, using an Olympus BX60 microscope with an UPlanFLN 40x/0.75 NA lens.

Statistics

Data are shown as means ± SEM, with the number of mice (n). Survival curves were compared using Kaplan-Meier followed by Log-rank analysis (Mantel-Cox) with Bonferroni correction for multiple comparisons. ANOVA followed by Tukey's post-hoc test for multiple comparisons was used to determine significant differences among groups for body weight, BAL cell and CFUs counts, MCC, BAL mucins content, BALF cytokines and immunoglobulin content, histology scores, and morphometric analyses. $p<0.05$ was considered statistically significant.

Supplementary Material

Refer to Web version on PubMed Central for supplementary material.

AKNOWLEDGEMENTS

The authors thank: Troy Rogers for assistance with mucociliary clearance studies; E. Jane Kelly and Danielle L. Waxer for technical assistance with mouse breeding, phenotyping and morphometric analyses; Dr. Michael Chua for assistance with imaging; Carlton W. Anderson of the UNC CGIBD's Advanced Analytics Core for performing the Multiplex assay;and Alexandra C. Infanzon for editorial assistance.

This work was funded by the Cystic Fibrosis Research Development Program grant RDP CFF R026-CR11 to W.K.O. and the CFF RDP BOUCHE15R0 to R.C.B, the National Institute of Health (NIH) P30-DK065988, P50-HL060280, P50-HL084934, P50-HL107168, P01-HL108808, P01-HL110873 and UH2-HL123645 (to R.C.B.). The UNC CGIBD's Advanced Analytics Core is supported by NIH grant P30 DK34987.

Drs. Boucher, Grubb, and O'Neal are inventors in US Patent US 7,772,458 B2 for the *Scnn1b*-Tg mouse model.

REFERENCES

1. Linden SK, Sutton P, Karlsson NG, Korolik V, McGuckin MA. Mucins in the mucosal barrier to infection. Mucosal immunology. 2008; 1:183–197. [PubMed: 19079178]
2. Anderson WH, et al. The Relationship of Mucus Concentration (Hydration) to Mucus Osmotic Pressure and Transport in Chronic Bronchitis. Am J Respir Crit Care Med. 2015; 192:182–190. doi: 10.1164/rccm.201412-2230OC. [PubMed: 25909230]
3. Henderson AG, et al. Cystic fibrosis airway secretions exhibit mucin hyperconcentration and increased osmotic pressure. The Journal of clinical investigation. 2014; 124:3047–3060. doi: 10.1172/JCI73469. [PubMed: 24892808]
4. Button B, et al. A periciliary brush promotes the lung health by separating the mucus layer from airway epithelia. Science. 2012; 337:937–941. [PubMed: 22923574]
5. Garcia MA, Yang N, Quinton PM. Normal mouse intestinal mucus release requires cystic fibrosis transmembrane regulator-dependent bicarbonate secretion. J Clin Invest. 2009; 119:2613–2622. doi: 10.1172/JCI38662. [PubMed: 19726884]
6. Gustafsson JK, et al. Bicarbonate and functional CFTR channel are required for proper mucin secretion and link cystic fibrosis with its mucus phenotype. The Journal of experimental medicine. 2012; 209:1263–1272. doi:10.1084/jem.20120562. [PubMed: 22711878]
7. Tang XX, et al. Acidic pH increases airway surface liquid viscosity in cystic fibrosis. J Clin Invest. 2016; 126:879–891. doi:10.1172/JCI83922. [PubMed: 26808501]
8. Shah VS, et al. Airway acidification initiates host defense abnormalities in cystic fibrosis mice. Science. 2016; 351:503–507. doi:10.1126/science.aad5589. [PubMed: 26823428]
9. Kesimer M, et al. Molecular organization of the mucins and glycocalyx underlying mucus transport over mucosal surfaces of the airways. Mucosal immunology. 2013; 6:379–392. doi:10.1038/mi. 2012.81. [PubMed: 22929560]
10. Kesimer M, Makhov AM, Griffith JD, Verdugo P, Sheehan JK. Unpacking a gel-forming mucin: a view of MUC5B organization after granular release. Am J Physiol Lung Cell Mol Physiol. 2010; 298:L15–22. doi:10.1152/ajplung.00194.2009. [PubMed: 19783639]
11. Kiwamoto T, et al. Endogenous airway mucins carry glycans that bind Siglec-F and induce eosinophil apoptosis. J Allergy Clin Immunol. 2015; 135:1329–1340. e1329. doi:10.1016/j.jaci. 2014.10.027. [PubMed: 25497369]
12. McDole JR, et al. Goblet cells deliver luminal antigen to CD103+ dendritic cells in the small intestine. Nature. 2012; 483:345–349. doi:10.1038/nature10863. [PubMed: 22422267]
13. Shan M, et al. Mucus enhances gut homeostasis and oral tolerance by delivering immunoregulatory signals. Science. 2013; 342:447–453. doi:10.1126/science.1237910. [PubMed: 24072822]
14. Thornton DJ, Sheehan JK. From Mucins to Mucus: Toward a More Coherent Understanding of This Essential Barrier 10.1513/pats.2306016. Proc Am Thorac Soc. 2004; 1:54–61. [PubMed: 16113413]
15. Kirkham S, Sheehan JK, Knight D, Richardson PS, Thornton DJ. Heterogeneity of airways mucus: variations in the amounts and glycoforms of the major oligomeric mucins MUC5AC and MUC5B. The Biochemical journal. 2002; 361:537–546. [PubMed: 11802783]
16. Thornton DJ, Rousseau K, McGuckin MA. Structure and function of the polymeric mucins in airways mucus. Annu Rev Physiol. 2008; 70:459–486. doi:10.1146/annurev.physiol. 70.113006.100702. [PubMed: 17850213]
17. Rose MC, Voynow JA. Respiratory tract mucin genes and mucin glycoproteins in health and disease. Physiol Rev. 2006; 86:245–278. [PubMed: 16371599]
18. Kirkham S, et al. MUC5B is the major mucin in the gel phase of sputum in chronic obstructive pulmonary disease. Am J Respir Crit Care Med. 2008; 178:1033–1039. doi:10.1164/rccm. 200803-391OC. [PubMed: 18776153]
19. Roy MG, et al. Muc5b is required for airway defence. Nature. 2014; 505:412–416. doi:10.1038/ nature12807. [PubMed: 24317696]
20. Evans CM, et al. The polymeric mucin Muc5ac is required for allergic airway hyperreactivity. Nature communications. 2015; 6:6281. doi:10.1038/ncomms7281.

21. Mall M, Grubb BR, Harkema JR, O'Neal WK, Boucher RC. Increased airway epithelial Na+ absorption produces cystic fibrosis-like lung disease in mice. Nat Med. 2004; 10:487–493. doi: 10.1038/nm1028. [PubMed: 15077107]
22. Livraghi-Butrico A, et al. Genetically determined heterogeneity of lung disease in a mouse model of airway mucus obstruction. Physiol Genomics. 2012; 44:470–484. [PubMed: 22395316]
23. O'Neal WK, et al. Assessment of genetic modifiers for phenotypic severity of Scnn1b-transgenic mice. Pediatric Pulmunology. 2007; (Supplement 30)
24. Mall MA, et al. Development of chronic bronchitis and emphysema in beta-epithelial Na+ channel-overexpressing mice. Am J Respir Crit Care Med. 2008; 177:730–742. doi:10.1164/rccm.200708-1233OC. [PubMed: 18079494]
25. Livraghi A, et al. Airway and lung pathology due to mucosal surface dehydration in {beta}-epithelial Na+ channel-overexpressing mice: role of TNF-{alpha} and IL-4R{alpha} signaling, influence of neonatal development, and limited efficacy of glucocorticoid treatment. J Immunol. 2009; 182:4357–4367. doi:10.4049/jimmunol.0802557. [PubMed: 19299736]
26. Roy MG, et al. Mucin production during prenatal and postnatal murine lung development. Am J Respir Cell Mol Biol. 2011; 44:755–760. doi:10.1165/rcmb.2010-0020OC 10.1165/rcmb.2010-0020RC. [PubMed: 21653907]
27. Livraghi-Butrico A, et al. Mucus clearance, MyD88-dependent and MyD88-independent immunity modulate lung susceptibility to spontaneous bacterial infection and inflammation. Mucosal immunology. 2012; 5:397–408. doi:10.1038/mi.2012.17. [PubMed: 22419116]
28. Hasnain SZ, et al. Muc5ac: a critical component mediating the rejection of enteric nematodes. The Journal of experimental medicine. 2011; 208:893–900. doi:10.1084/jem.20102057. [PubMed: 21502330]
29. Foo SY, Phipps S. Regulation of inducible BALT formation and contribution to immunity and pathology. Mucosal immunology. 2010; 3:537–544. doi:10.1038/mi.2010.52. [PubMed: 20811344]
30. Phalipon A, et al. Secretory component: a new role in secretory IgA-mediated immune exclusion in vivo. Immunity. 2002; 17:107–115. [PubMed: 12150896]
31. Gilley SK, et al. Deletion of airway cilia results in noninflammatory bronchiectasis and hyperreactive airways. American journal of physiology. Lung cellular and molecular physiology. 2014; 306:L162–169. doi:10.1152/ajplung.00095.2013. [PubMed: 24213915]
32. Livraghi A, Randell SH. Cystic fibrosis and other respiratory diseases of impaired mucus clearance. Toxicologic Pathology. 2007; 35:116–129. [PubMed: 17325980]
33. Ostrowski LE, et al. Conditional deletion of dnaic1 in a murine model of primary ciliary dyskinesia causes chronic rhinosinusitis. American Journal of Respiratory Cell and Molecular Biology. 2010; 43:55–63. [PubMed: 19675306]
34. Zhu Y, et al. Munc13-2−/− baseline secretion defect reveals source of oligomeric mucins in mouse airways. J Physiol. 2008; 586:1977–1992. doi:10.1113/jphysiol.2007.149310. [PubMed: 18258655]
35. Rajavelu P, et al. Airway epithelial SPDEF integrates goblet cell differentiation and pulmonary Th2 inflammation. J Clin Invest. 2015; 125:2021–2031. doi:10.1172/JCI79422. [PubMed: 25866971]
36. Contreras-Ruiz L, Masli S. Immunomodulatory cross-talk between conjunctival goblet cells and dendritic cells. PLoS One. 2015; 10:e0120284. doi:10.1371/journal.pone.0120284. [PubMed: 25793763]
37. Knoop KA, McDonald KG, McCrate S, McDole JR, Newberry RD. Microbial sensing by goblet cells controls immune surveillance of luminal antigens in the colon. Mucosal immunology. 2015; 8:198–210. doi:10.1038/mi.2014.58. [PubMed: 25005358]
38. Kesimer M, et al. Tracheobronchial air-liquid interface cell culture: a model for innate mucosal defense of the upper airways? Am J Physiol Lung Cell Mol Physiol. 2009; 296:L92–L100. doi: 10.1152/ajplung.90388.2008. [PubMed: 18931053]
39. Radicioni G, et al. The innate immune properties of airway mucosal surfaces are regulated by dynamic interactions between mucins and interacting proteins: the mucin interactome. Mucosal immunology. 2016 doi:10.1038/mi.2016.27.

40. Corthesy B. Multi-faceted functions of secretory IgA at mucosal surfaces. Front Immunol. 2013; 4:185. doi:10.3389/fimmu.2013.00185. [PubMed: 23874333]

41. Lee SH, et al. Increased expression of vascular endothelial growth factor and hypoxia inducible factor-1alpha in lung tissue of patients with chronic bronchitis. Clin Biochem. 2014; 47:552–559. doi:10.1016/j.clinbiochem.2014.01.012. [PubMed: 24463065]

42. Ehre C, et al. Overexpressing mouse model demonstrates the protective role of Muc5ac in the lungs. Proceedings of the National Academy of Sciences of the United States of America. 2012; 109:16528–16533. doi:10.1073/pnas.1206552109. [PubMed: 23012413]

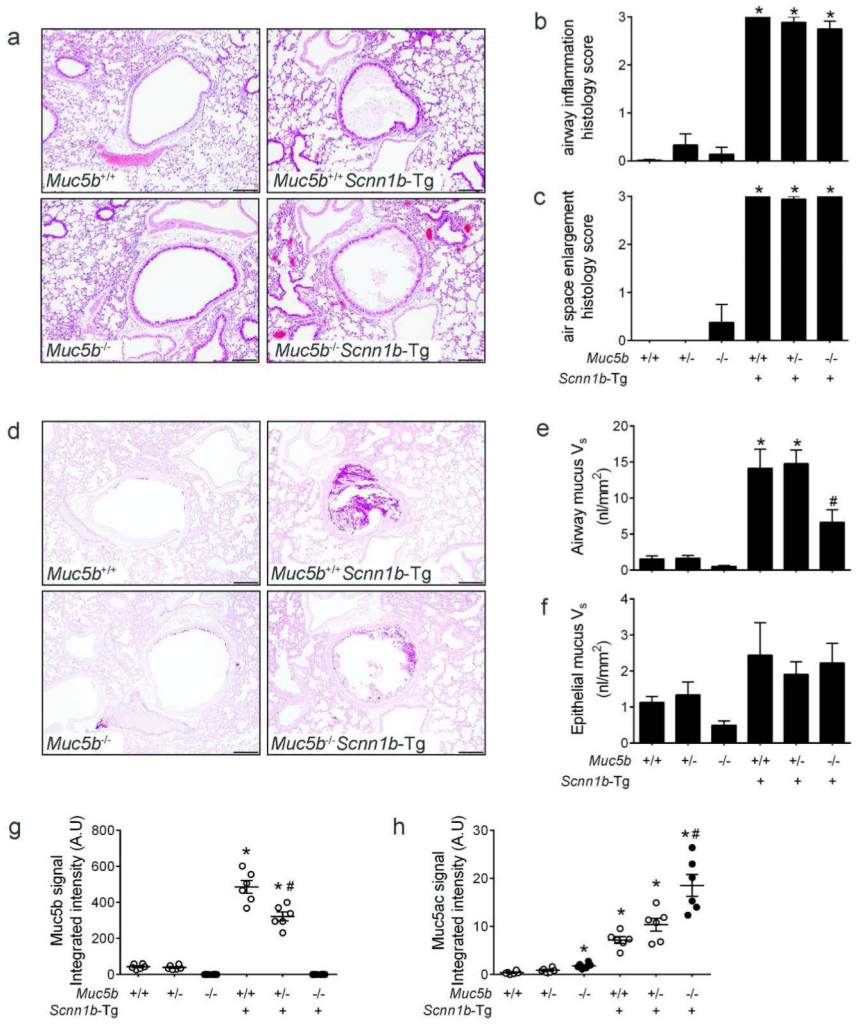

Figure 1. Mucus hyperconcentration/adhesion is necessary to produce bronchitic lung pathology, but Muc5b deletion ameliorates airway mucus obstruction in *Scnn1b*-Tg mice

(**a**) Representative photomicrographs of airway lumens cut in cross section proximal to the hilum from PND35 mice of the indicated genotypes, stained with H&E illustrating airway mucus obstruction and inflammatory infiltrates characteristic of bronchitic lung pathology in *Scnn1b*-Tg mice. (**b-c**) Semi-quantitative histology scores for airway inflammation (**b**) and air space enlargement (**c**) in PND35 mice from the *Muc5b*$^{-/-}$ × *Scnn1b*-Tg cross in the C57:129 genetic background. n= 6-9 mice/genotype. ANOVA * p<0.05 vs. *Muc5b*$^{+/+}$ mice. (**d**) Equivalent sections as in (**a**) stained with AB-PAS for mucopolysaccharides, illustrating significant amelioration of mucus obstruction in *Muc5b*$^{-/-}$ *Scnn1b*-Tg vs. *Muc5b*$^{+/+}$ *Scnn1b*-Tg mice. Scale bar 0.1 mm. (**e-f**) Morphometric analysis of total (epithelial+luminal, **e**) and epithelial (**f**) airway mucus volume density (V_s) in PND35 mice (C57:129 genetic background). n= 6-9 mice/genotype. ANOVA * p<0.05 vs. *Muc5b*$^{+/+}$ mice, # p<0.05 vs. *Muc5b*$^{+/+}$ *Scnn1b*-Tg mice. (**g-h**) Densitometric analysis of mucin agarose western blots of BAL from the progeny of the *Muc5b*$^{-/-}$ × *Scnn1b*-Tg cross in the C57 congenic background, at PND35. Blots were probed with anti-Muc5b (**g**) or anti-Muc5ac (**h**)

antibodies. n=6 mice/genotype. ANOVA * $p<0.05$ vs. *Muc5b*$^{+/+}$ mice, # $p<0.05$ vs. *Muc5b*$^{+/+}$ *Scnn1b*-Tg mice.

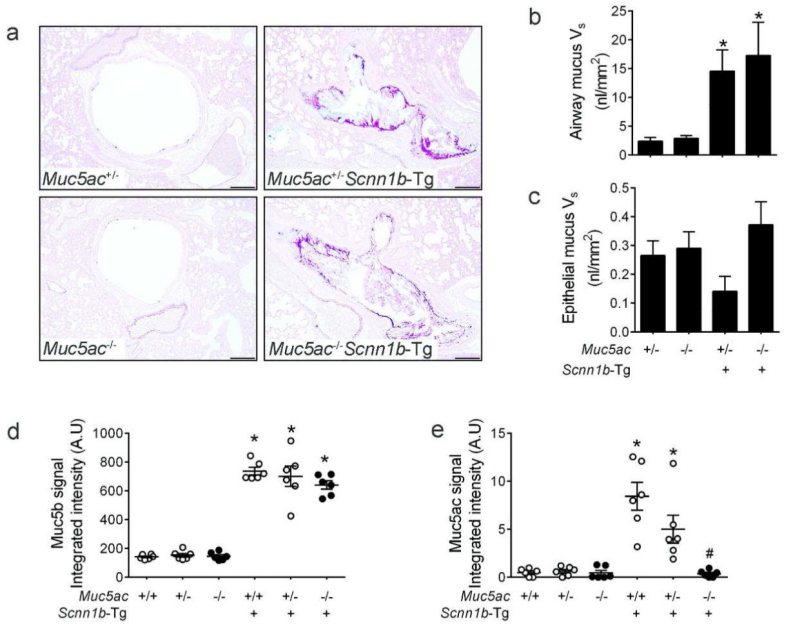

Figure 2. Muc5ac deletion does not ameliorate airway mucus obstruction in *Scnn1b*-Tg mice

(**a**) Representative photomicrographs of proximal left lobe main stem bronchus from PND35 mice of the indicated genotypes, stained with AB-PAS for mucopolysaccharides, illustrating no changes in mucus obstruction in *Muc5ac*$^{-/-}$ *Scnn1b*-Tg vs. *Muc5ac*$^{+/-}$ *Scnn1b*-Tg mice. Scale bar 0.1 mm. (**b-c**) Morphometric analysis of total (epithelial+luminal, **b**) and epithelial (**c**) airway mucus volume density (V_s) in PND35 mice (C57:129 genetic background). n= 6-11 mice/genotype. ANOVA * $p<0.05$ vs. *Muc5ac*$^{+/+}$ mice. (**d-e**) Densitometric analysis of mucin agarose western blots of BAL from the progeny of the *Muc5ac*$^{-/-}$ × *Scnn1b*-Tg cross in the C57 congenic background, at PND35. Blots were probed with anti-Muc5b (**d**) or anti-Muc5ac (**e**) antibodies. n= 6 mice/genotype. ANOVA * $p<0.05$ vs. *Muc5ac*$^{+/+}$ mice, # $p<0.05$ vs. *Muc5ac*$^{+/+}$ *Scnn1b*-Tg mice.

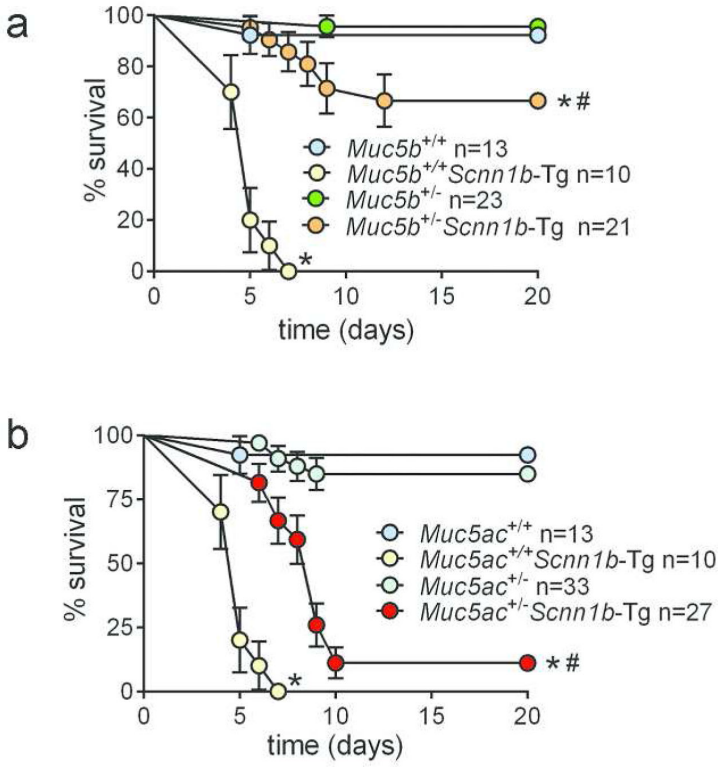

Figure 3. Relative contribution of Muc5ac vs. Muc5b to neonatal survival in a model of lethal mucus obstruction, the F1 C57:FVB/NJ *Scnn1b*-Tg mice

Survival curves for the progeny of the *Muc5b*$^{-/-}$ *Scnn1b*-Tg mice (**a**) or *Muc5ac*$^{-/-}$ *Scnn1b*-Tg mice (**b**) crossed with inbred FVB/NJ mice. Muc5b heterozygosity improved overall survival of F1 C57:FVB *Scnn1b*-Tg mice, whereas Muc5ac heterozygosity only resulted in delayed time of death (median survival PND 9 vs. PND 5 for *Muc5ac*$^{+/-}$ *Scnn1b*-Tg mice vs. *Muc5ac*$^{+/+}$ *Scnn1b*-Tg mice, respectively). * $p<0.05$ vs. *Muc*$^{+/+}$ littermates, # $p<0.05$ vs. *Muc*$^{+/+}$ *Scnn1b*-Tg littermates.

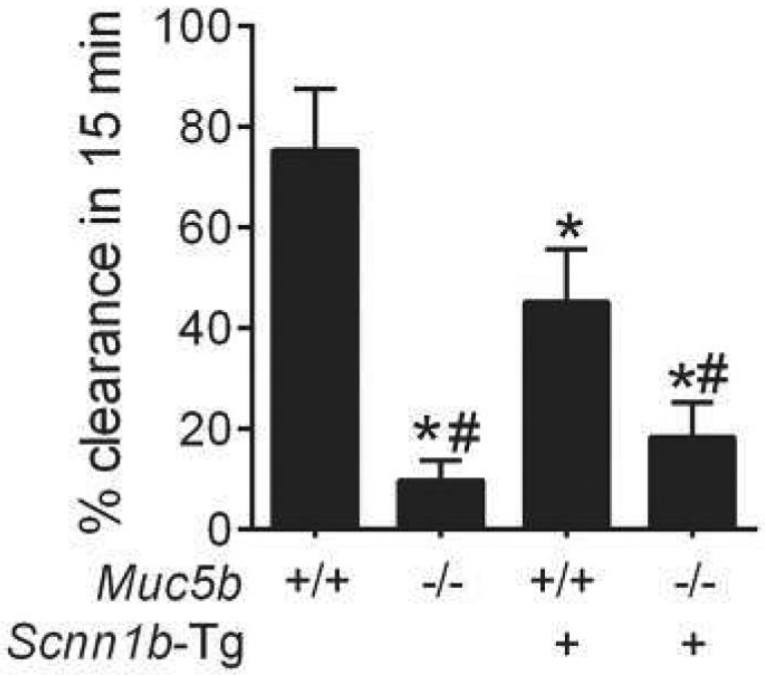

Figure 4. Mucociliary transport only partially correlates with the severity of muco-obstructive lung disease

Mucociliary clearance measurements in selected genotypes from the progeny of the *Muc5b*$^{-/-}$ × *Scnn1b*-Tg cross in the C57 congenic background, at PND35. n=6-14 mice/genotype. ANOVA * $p<0.05$ vs. *Muc5b*$^{+/+}$ mice, # $p<0.05$ vs. *Muc5b*$^{+/+}$ *Scnn1b*-Tg mice.

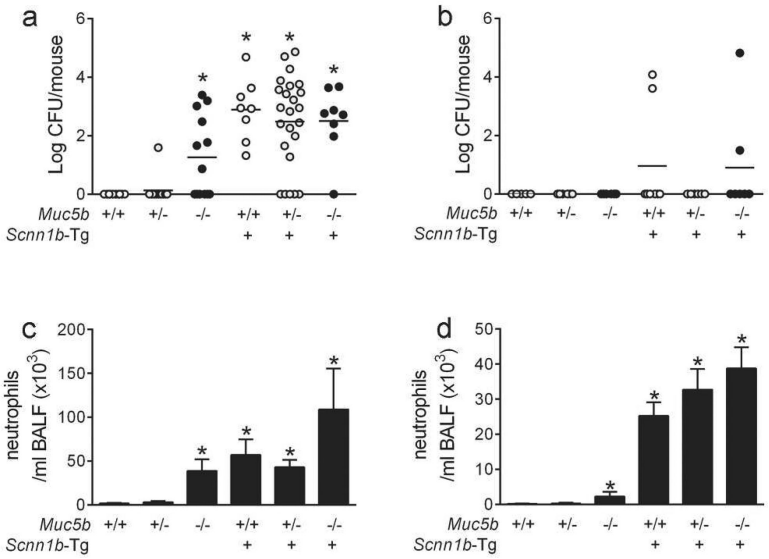

Figure 5. Deletion of Muc5b or Muc5ac does not affect bacterial burden or ameliorate airway inflammation in *Scnn1b*-Tg mice

(**a,b**) Quantification of colony forming units (CFU) in BAL samples from the progeny of the *Muc5b*$^{-/-}$ × *Scnn1b*-Tg cross in the C57:129 genetic background, at PND5-7 (**a**) or PND35 (**b**). (Log_{10}+1)-transformed data. n= 8-24 mice/genotype (a) and n=5-8 mice/genotype (b). ANOVA * p<0.05 vs. *Muc5b*$^{+/+}$ mice. (**c-d**) BAL neutrophil counts for the progeny of the *Muc5b*$^{-/-}$ × *Scnn1b*-Tg cross in the C57:129 genetic background, at PND5-7 (**c**) or PND35 (**d**) n= 7-24 mice/genotype (c) and n=11-15 mice/genotype (d). ANOVA * p<0.05 vs. *Muc5b*$^{+/+}$ mice.

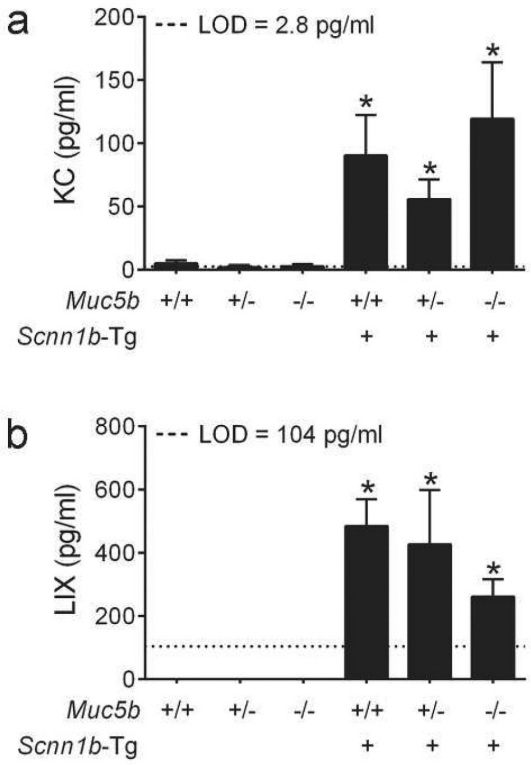

Figure 6. Deletion of Muc5b does not alter the BAL chemokine and cytokine profile in *Scnn1b*-Tg mice

KC (**a**) and LIX (**b**) levels in cell-free BAL from the progeny of the *Muc5b*$^{-/-}$ × *Scnn1b*-Tg cross in the C57:129 genetic background at PND35. The dotted line represents the assay lower detection limit (LOD). n= 5-8 mice/genotype. ANOVA * $p<0.05$ vs. *Muc5b*$^{+/+}$ mice.

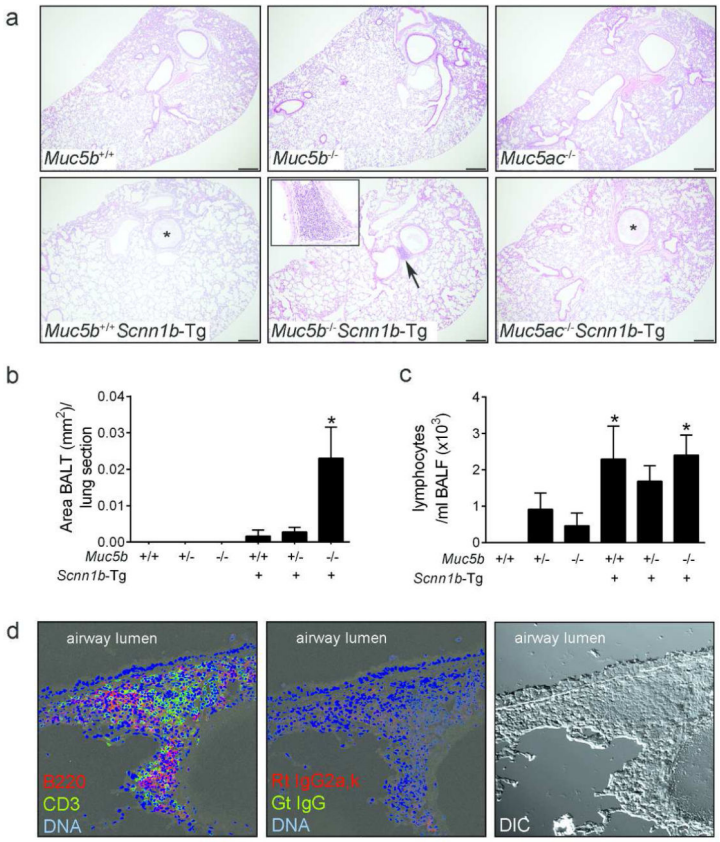

Figure 7. Deletion of Muc5b, but not Muc5ac, worsens the incidence of bronchus-associated lymphoid tissue (BALT) in *Scnn1b*-Tg mice

(**a**) Representative micrographs of proximal left lobe main stem bronchus from PND35 mice, stained with H&E, illustrating typical histopathology for the indicated genotypes. Scale bar 0.2 mm. Airway mucus obstruction was evident in *Muc5b*$^{+/+}$*Scnn1b*-Tg mice and *Muc5ac*$^{-/-}$*Scnn1b*-Tg mice (asterisks), but it was less severe in *Muc5b*$^{-/-}$*Scnn1b*-Tg mice. However, *Muc5b*$^{-/-}$*Scnn1b*-Tg mice presented with a higher incidence of BALT (arrow and high magnification inset, scale bar 20 μm). (**b**) Morphometric analysis of BALT in PND35 mice (C57:129 genetic background). n= 6-9 mice/genotype. ANOVA * $p<0.05$ vs. *Muc5b*$^{+/+}$ mice. (**c**) BAL lymphocyte counts for the progeny of the *Muc5b*$^{-/-}$ × *Scnn1b*-Tg cross in the C57:129 genetic background, at PND35. n= 11-15 mice/genotype. ANOVA * $p<0.05$ vs. *Muc5b*$^{+/+}$ mice. (**d**) Representative confocal images of BALT immunostained with B and T cells specific markers (B220 in red and CD3 in green, respectively), and relevant isotype negative controls (rat IgG2a,k and goat IgG, respectively). Nuclei are stained in blue (DAPI). Differential interference contrast (DIC) image is provided to illustrate the typical localization of BALT in the airway submucosal compartment.

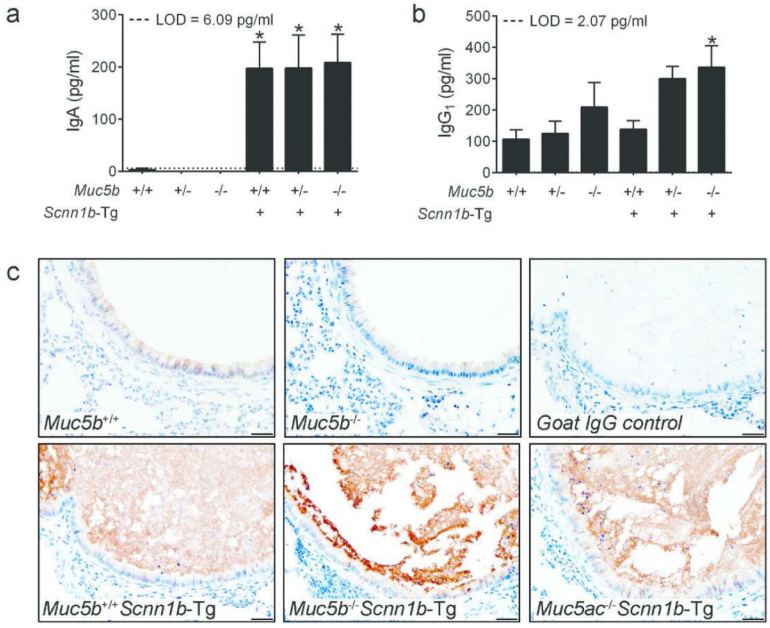

Figure 8. Airway mucus hyperconcentration/adhesion stimulates IgA secretion

(**a,b**) IgA (**a**) and IgG_1 (**b**) levels in cell-free BAL from the progeny of the *Muc5b*$^{-/-}$ × *Scnn1b*-Tg cross in the C57:129 genetic background at PND35. The dotted line represents the assay lower detection limit (LOD). n= 5-8 mice/genotype. ANOVA * $p<0.05$ vs. *Muc5b*$^{+/+}$ mice. (**c**) Immunohistochemical localization of the polymeric Ig receptor secretory component (SC) in the main stem bronchus of mice for the indicated genotypes. A serial section to the one used for *Muc5b*$^{+/+}$ *Scnn1b*-Tg SC stain is shown as negative IgG control (IgG control).